

Model-Fitting Approach to Kinetic Analysis of Non-Isothermal Oxidation of Molybdenite

Ebrahimi Kahrizsangi, Reza⁺; Abbasi, Mohammad Hasan; Saidi, Ali*

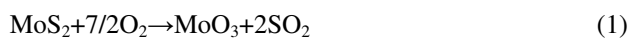
Department of Materials Engineering, Isfahan University of Technology, Isfahan, I.R. IRAN

ABSTRACT: *The kinetics of molybdenite oxidation was studied by non-isothermal TGA-DTA with heating rate 5 °C.min⁻¹. The model-fitting kinetic approach applied to TGA data. The Coats-Redfern method used for model fitting. The popular model-fitting gives excellent fit for non-isothermal data in chemically controlled regime. The apparent activation energy was determined to be about 34.2 kcalmol⁻¹ with pre-exponential factor about 10⁸ sec⁻¹ for extent of reaction less than 0.5.*

KEY WORDS: *Kinetics, Molybdenite, Non-isothermal, Model-fitting, TGA, DTA.*

INTRODUCTION

The main industrial method of processing molybdenite is its oxidized roasting in air atmosphere [1,2]. This is based on the oxidation of molybdenite to technical molybdc oxide (MoO₃) which is the starting material for most of the molybdenium products. The roasting of molybdenite concentrate involves a number of chemical reactions. In the main reaction molybdenite reacts rapidly and exothermically with oxygen and yields Molybdenum trioxide



The heat of reaction being about -252 kcalmol⁻¹ of MoS₂ at 600 °C. The reaction is virtually irreversible and takes place even at very low concentrations of oxygen in the gaseous phase. There are only two papers in the literature [3,4] about the kinetics of molybdenite oxidation. Both of them have been done in the isothermal condition and in this paper we focus on the kinetic analysis of non-isothermal data. The kinetics of molybdenite oxidation

can be studied by thermogravimetry method. Although kinetics studies can be performed in very different devices, thermogravimetry (TG) is the most used technique [5]. In a TG experiment, a modern equipment typically registers hundreds or thousands of experimental points, usually total weight (or a related magnitude), temperature and time. Temperature and time are related by a 'program' set by the user. Although the equipment control system tries to adjust the actual temperature to fit the programmed one, some times important differences appear (for example due to endothermic or exothermic reactions).

EXPERIMENTAL

This research was carried out with molybdenite samples from the Sarcheshmeh copper industry in Iran with 1.3 m²gr⁻¹ specific surface area and particle size in the range of 60-80 μm. The chemical composition of the studied molybdenite was Mo (55.9 %), Cu (1.1 %), and S (39 %).

* To whom correspondence should be addressed.

+ E-mail: rezaebrahimi@iaun.ac.ir

1021-9986/07/2/119

5/\$/2.50

Table 1: Solid state reaction rate models.

Reaction Model	f(α)	g(α)
Nucleation models		
Power Law	$4\alpha^{3/4}$	$\alpha^{1/4}$
Power Law	$3\alpha^{2/3}$	$\alpha^{1/3}$
Power Law	$2\alpha^{1/2}$	$\alpha^{1/2}$
Avrami-Erofeev	$4(1-\alpha)[- \ln(1-\alpha)]^{3/4}$	$[- \ln(1-\alpha)]^{1/4}$
Avrami-Erofeev	$3(1-\alpha)[- \ln(1-\alpha)]^{2/3}$	$[- \ln(1-\alpha)]^{1/3}$
Avrami-Erofeev	$2(1-\alpha)[- \ln(1-\alpha)]^{1/2}$	$[- \ln(1-\alpha)]^{1/2}$
Diffusion models		
One dimensional Diffusion	$1/2\alpha^{-1}$	α^2
Diffusion control (Janders)	$2(1-\alpha)^{2/3}[1-(1-\alpha)^{1/3}] - 1$	$[1-(1-\alpha)^{1/3}]^2$
Diffusion control (Crank)	$3/2[(1-\alpha)^{-1/3} - 1]^{-1}$	$1-2/3\alpha - (1-\alpha)^{2/3}$
Reaction order and geometrical contraction models		
Mampel (first order)	$1-\alpha$	$-\ln(1-\alpha)$
Second Order	$(1-\alpha)^2$	$(1-\alpha)^{-1} - 1$
Contracting cylinder	$2(1-\alpha)^{1/2}$	$1 - (1-\alpha)^{1/2}$
Contracting Sphere	$3(1-\alpha)^{2/3}$	$1 - (1-\alpha)^{1/3}$

A Mettler Tuledu Star System was used for simultaneous TGA-DTA studies. Experiments were performed under non-isothermal condition at programmed linear heating rate of $5\text{ }^\circ\text{Cmin}^{-1}$. Oxygen flowing was used for molybdenite oxidation with flow rate maintained at 50 ml.min^{-1} . The starting material and products were analyzed by employing Philips X-pert X-Ray diffractometer with PW 2273 tube and Cu K α radiation with scan rate $0.04\text{ }^\circ\text{C.sec}^{-1}$. The models fitted for extent of reaction less than 0.5.

Rate law and kinetics analysis

The rate of a solid state reaction can be generally described by:

$$\frac{d\alpha}{dt} = k(T)f(\alpha) \quad (2)$$

Where t is the time, T is the temperature, α is the extent of reaction and f(α) is reaction model. Integration of the above equation gives the integral rate law:

$$g(\alpha) = kt \quad (3)$$

Where g(α) is the integral reaction model. Several reaction models [6] using f(α) or g(α) are listed in table 1.

The explicit temperature dependence of the rate constant is introduced by replacing k(T) with the Arrhenius equation which gives:

$$\frac{d\alpha}{dt} = A \exp\left(\frac{-Ea}{RT}\right)f(\alpha) \quad (4)$$

$$g(\alpha) = A \exp\left(\frac{-Ea}{RT}\right)t \quad (5)$$

Where A (the pre-exponential factor) and E (activation energy) are the Arrhenius parameters and R is the gas constant. The Arrhenius parameters together with the reaction model are sometimes called the kinetics triplet. Under non-isothermal condition in which a sample heated at a constant rate, the explicit temporal in eq. (4) is eliminated through the trivial transformation:

$$\frac{d\alpha}{dT} = \frac{A}{\beta} \exp\left(\frac{-Ea}{RT}\right)f(\alpha) \quad (6)$$

Where β is the heating rate. Upon integration, eq. (6) gives:

$$g(\alpha) = \frac{A}{\beta} \int_0^T e^{\left(\frac{-Ea}{RT}\right)} dT \quad (7)$$

If Ea/RT is replaced by x and integration limits transformed, eq. (7) becomes,

$$g(\alpha) = \frac{AEa}{RT} \int_x^\infty \frac{e^{-x}}{x^2} dx \quad (8)$$

eq. (8) can be written as

$$g(\alpha) = \frac{AEa}{RT} p(x) \quad (9)$$

Where $p(x)$ is the exponential integral. The $p(x)$ has no analytical solution but has many approximations [7]. Kinetics parameters can be obtained from non-isothermal rate laws by both model-fitting and isoconversional (model-free) methods [8,9].

Model-fitting methods involve fitting different models to α -temperature curves and simultaneously determining the activation energy (E) and frequency factor (A). There are several non-isothermal model-fitting methods. One of the most popular being the Coats and Redfern method [10]. This method utilizes the asymptotic series expansion for approximating the exponential integral in eq. (9) giving.

$$\ln \frac{g(\alpha)}{T^2} = \ln \left[\frac{AR}{\beta Ea} \left(1 - \frac{2R\bar{T}}{Ea} \right) \right] - \frac{Ea}{RT} \quad (10)$$

Where \bar{T} is the mean experimental temperature. Plotting the left hand side of eq. (10), which includes the model $g(\alpha)$ versus $1/T$ gives Ea and A from the slope and intercept respectively. The model that gives the best linear fit is selected as the chosen model.

RESULTS AND DISCUSSION

XRD pattern of the studied Molybdenite concentrate with characteristic peaks of MoS_2 is shown in Fig. 1. No mineral impurity was detected in the concentrate. Fig. 2 shows the simultaneous TGA and DTA curves for molybdenite oxidation and in Fig. 3 the DTG and DTA curves are shown where these curves show similar trend. Figs. 2 and 3 demonstrate that molybdenite oxidation begins at 350 °C as indicated by the small peak at DTA curve. This is followed by a large exothermic peak with a maximum at 485 °C representing intensive oxidation of molybdenite. The point E in Fig 2 shows the end of molybdenite oxidation. At this point, decrease in the weight of sample is 10.43 % that shows a little difference

with 10 % weight loss for complete oxidation of molybdenite to MoO_3 . This difference may be due to sample purity and/or formation of MoO_2 during oxidation. After the oxidation of Molybdenite there is some reduction in sample weight. This reduction is due to MoO_3 sublimation. Fig. 4 shows the XRD pattern of TGA product at the end stage of mass decreasing and represent that almost all of the product is MoO_3 .

Using the TGA data the extent of reaction was calculated by the following equation.

$$\alpha = \frac{w_0 - w_t}{Bw_0} \quad (11)$$

Where w_0 and w_t are the masses of the sample initially and at time t respectively, and B is the fraction of weight loss for complete oxidation of MoS_2 to MoO_3 ($B=0.1$). In this study the weight of TGA sample at 350 °C is considered as w_0 . By inserting various $g(\alpha)$ into eq. (10) Arrhenius parameters was determined from the plot $\ln(g(\alpha)/T^2)$ against T^{-1} . The set of Arrhenius parameters for Molybdenite oxidation are shown in table 2.

For each model the goodness of fit is customarily estimated by a coefficient of linear correlation, r . A single pair of E and A is then commonly chosen as that corresponding to a reaction model that gives rise to the maximum absolute value of the correlation coefficient, $|r_{max}|$ [11-14]. As seen from table 2 all reaction models have correlation coefficient greater than 0.9. From the view point of pre-exponential factors for the solid state reactions the theoretical values are 10^6 - 10^{18} sec^{-1} , [15].

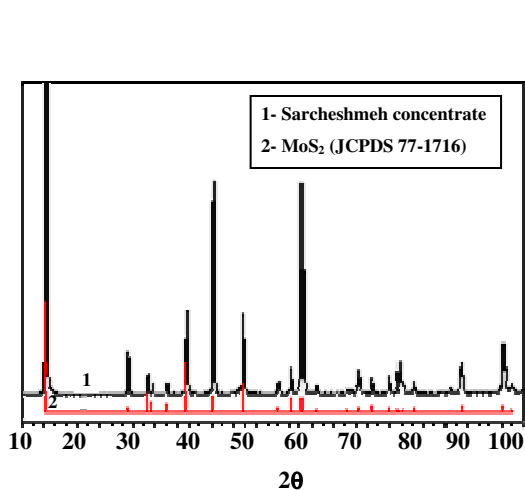
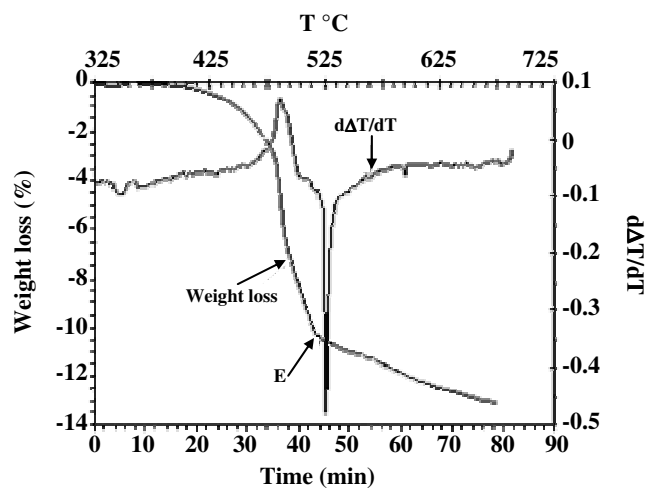
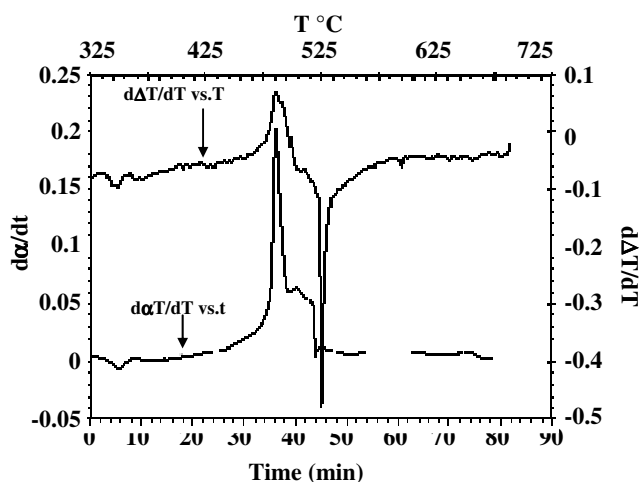
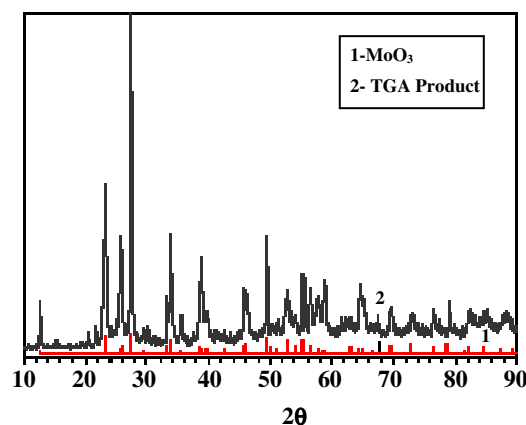
In table 2 all nucleation models (1-6) have very small pre-exponential factors indicating that these models can not explain the reaction mechanism. Among the remaining models the chemically controlled models (10-13) have maximum absolute value of the correlation coefficient thus these models could be the reaction models and the apparent activation energy for the Molybdenite oxidation in the chemically controlled step is $34.2 \text{ kcal.mol}^{-1}$ with pre-exponential factor about 10^8 sec^{-1} . This value is equal to Abdel-Rehim work [4] in the isothermal oxidation of Molybdenite at 450 °C.

CONCLUSIONS

Thermal analysis of Molybdenite oxidation has demonstrated that its oxidation begins at 350 °C, as indicated by the small peak at such temperature. This is

Table 2: Arrhenius parameters for non-isothermal oxidation of Molybdenite determined using the Coats-Redfern equation.

Model	$g(\alpha)$	E (kcal.mol ⁻¹)	A (sec ⁻¹)	-r
1	$\alpha^{1/4}$	8	4.25	0.9235
2	$\alpha^{1/3}$	9.2	17.5	0.9145
3	$\alpha^{1/2}$	15.17	1.75	0.9015
4	$[-\ln(1-\alpha)]^{1/4}$	6.48	2.81	0.9264
5	$[-\ln(1-\alpha)]^{1/3}$	9.56	23.73	0.9084
6	$[-\ln(1-\alpha)]^{1/2}$	15.73	1.68×10^3	0.9321
7	α^2	69	2.37×10^{18}	0.9421
8	$[1-(1-\alpha)^{1/3}]^2$	70.48	8.23×10^{17}	0.9361
9	$1-2/3 \alpha - (1-\alpha)^{2/3}$	70	5.6×10^{17}	0.9325
10	$-\ln(1-\alpha)$	34.23	4.1×10^8	0.9994
11	$(1-\alpha)^{-1} - 1$	35.39	1.03×10^9	0.9993
12	$1 - (1-\alpha)^{1/2}$	33.67	1.3×10^8	0.9993
13	$1 - (1-\alpha)^{1/3}$	33.85	1.03×10^8	0.9994

Fig. 1: XRD pattern of molybdenite concentrate with MoS₂ characteristic peaks.Fig. 2: TGA and DTA curves of molybdenite oxidation. Mass of sample 30 mg; heating rate 5 °C min⁻¹.Fig. 3: DTG and DTA curves of Molybdenite oxidation. Heating rate 5 °C min⁻¹.Fig. 4: XRD pattern of TGA products with MoO₃ characteristic peaks.

followed immediately by a large, wide exothermic peak at 485 °C representing the intensive oxidation of molybdenite.

The model-fitting method was applied to non-isothermal data of Molybdenite oxidation and the Coats-Redfern method was used for model fitting. The experimental data reveal that the rate of the reaction of Molybdenite oxidation is chemically rate determining for the extent of reaction less than 0.5.

Received : 5th November 2005 ; Accepted : 9th October 2006

REFERENCES

- [1] Gupta, C.K., Extractive Metallurgy of Molybdenum, CRC Press, USA (1992).
- [2] Abdel-Rehim, A. M., *J. Thermal Anal.*, **46**, 193, (1996).
- [3] Wilkomirsky, I.A., Watkinson, A.P., Brimacombe, J.K., *Transactions of the Institution of Mining & Metallurgy, Section C*, **86**, 16, (1977).
- [4] Abdel-Rehim, A. M., *J. of Therm. Anal. And Cal.*, **57**, 415, (1999).
- [5] Caballero, J. A., Conesa, J. A., *J. Anal. Appl. Pyrolysis*, **86**, 85, (2005).
- [6] Galwey, A.K., Brown, M.E., Thermal Decomposition of Ionic Solids, Second Ed., Elsevier, Amsterdam, (1999).
- [7] Flynn, J.H., *Thermochimica Acta*, **300**, 83, (1997).
- [8] Polli, H., Pontes, L.A.M. Araujo, A.S., *J. of Therm. Anal. and Cal.*, **79**, 383 (2005).
- [9] Khawam, A., Flangan, D.R., *Thermochimica Acta*, **436**, 101, (2005).
- [10] Vyazovkin, S., Wight, C.A., *Thermochimica Acta*, **340**, 53 (1999).
- [11] Sun, T., Zhao, Y., *J. Therm. Anal.*, **45**, 1105, (1995).
- [12] Yang, Z. H., Li, X. Y., *J. Therm. Anal.*, **48**, 917, (1997).
- [13] Hu, P., Cui, X.G., *J. Therm. Anal.*, **48**, 1379, (1997).
- [14] Budrugaec, E., *J. Therm. Anal.*, **49**, 183, (1997).
- [15] Vyazovkin, S., Wight, C.A., *Int. Rev. In Phy. Chem.*, **17**, 407, (1998).